

Dartmouth College

Dartmouth Digital Commons

Dartmouth Scholarship

Faculty Work

3-25-1983

Evidence for Hydrated Spermidine-Calf Thymus DNA Toruses Organized by Circumferential DNA Wrapping

Kenneth A. Marx
Dartmouth College

George C. Ruben
Dartmouth College

Follow this and additional works at: <https://digitalcommons.dartmouth.edu/facoa>



Part of the [Life Sciences Commons](#), and the [Medicine and Health Sciences Commons](#)

Dartmouth Digital Commons Citation

Marx, Kenneth A. and Ruben, George C., "Evidence for Hydrated Spermidine-Calf Thymus DNA Toruses Organized by Circumferential DNA Wrapping" (1983). *Dartmouth Scholarship*. 3830.
<https://digitalcommons.dartmouth.edu/facoa/3830>

This Article is brought to you for free and open access by the Faculty Work at Dartmouth Digital Commons. It has been accepted for inclusion in Dartmouth Scholarship by an authorized administrator of Dartmouth Digital Commons. For more information, please contact dartmouthdigitalcommons@groups.dartmouth.edu.

Evidence for hydrated spermidine-calf thymus DNA toruses organized by circumferential DNA wrapping

Kenneth A. Marx* and George C. Ruben +

Department of Chemistry, Dartmouth College and + Department of Pathology, and Norris Cotton Cancer Center, Dartmouth Medical School, Hanover, NH 03755, USA

Received 29 November 1982; Revised and Accepted 17 February 1983

ABSTRACT

In spermidine-condensed calf thymus DNA preparations, torus-shaped condensates were shown by transmission electron microscopy to exist under the hydrated conditions of the freeze fracture experiment. Using extremely low Pt metal deposition levels (9 Å Pt/C) high-contrast replicas of the spermidine-DNA toruses were obtained that showed circumferential wrapping of single DNA double helix-size surface fibres. Stereoscopic analysis of high magnification stereomicrographs established some details of the three-dimensional organization of two DNA double helix sections winding circumferentially on the inner surface of one such torus. These measurements demonstrate the usefulness of stereoscopic analysis of these high macromolecular organization magnification. Measurements on a number of torus-shaped complexes ($n=16$) yielded these average dimensions: inner circumference (1840 ± 204 Å), outer circumference (2800 ± 222 Å), torus ring thickness (143 ± 18 Å). These data support a continuous circumferential DNA-winding model of torus organization proposed by Marx & Reynolds¹.

INTRODUCTION

DNA has been shown to form condensed structures *in vitro* when cations with three or more positive charges are added to aqueous solution. These cations may be inorganic², organic polyamines¹⁻¹¹, or macromolecules, such as histones¹². This reversible DNA condensation phenomenon has been successfully described by Manning's counterion condensation theory¹³. When visualized in the electron microscope, dehydrated preparations of the cation-condensed DNA systems exhibit a variety of condensed DNA structures. Prominent among all structures found in these systems is the torus. Since polyamines occur in nature as major ionic constituents of virus and bacteriophage heads and since condensed DNA genomes having a torus-like organization have been visualized by transmission electron microscopy (TEM) in the negatively stained and dehydrated preparations of λ ⁴ and T-4^{14,15} bacteriophage and herpes simple virus,¹⁶ the *in vitro* polyamine-condensed DNA torus represents a valuable model system for studying DNA organization in the biological

structures.

Our preliminary freeze-etch TEM studies of spermidine-condensed calf thymus DNA preparations have demonstrated the existence of the torus geometry in a hydrated condition⁹. In this TEM study we present micrographs of a number of representative spermidine-condensed calf thymus DNA toruses prepared by the freeze-etch technique. Analyses of distributions of inner and outer torus circumference and torus ring thickness are presented. These data are consistent with a continuous circumferential DNA-wrapping model of torus organization which was developed to explain the arithmetic series of DNA fragment lengths produced upon micrococcal nuclease cleavage of the condensed structures in a previous study¹⁷. Direct visualization of circumferential DNA wrapping of up to half the torus circumference is shown for a number of these objects. Our analysis of high magnification stereo-micrographs of two torus-shaped spermidine-calf thymus DNA complexes further strengthens this interpretation. Using a mirror stereoscope with light-dot parallax device, we have mapped in three dimensions at different positions on the surface of one torus the circumferential winding of two putative DNA double helices around almost one half the torus circumference.

MATERIALS AND METHODS

We performed freeze-etch transmission electron microscopy (TEM) on samples of spermidine-condensed calf thymus DNA (5 µg/ml) complexes in 0.2 mM spermidine in 1 mM NaCl, 10mM Tris pH 7.0. The DNA fragment size was found to range in molecular weight from 10-20 x 10⁶d. A weight average fragment size of 13 x 10⁶d was determined from analysis of the fragment distribution in a 0.5% agarose gel. Samples were freeze-fractured and etched for 13 min at Balzers GA-1 setting of -97°C which is a sample temperature of -68°C. The replica was formed at a 45° angle with a Balzers 300 freezing microtome equipped with two EKV552 electron beam guns. A QSG 201 D Balzer's Quartz crystal thin film monitor was used to deposit the 9 Å Pt-C film, subsequently backed with a 65 Å thick carbon film at a Balzer's GA-1 setting of -150°C (2min) and a sample temperature of -73°C. The two EKV 552 electron beam guns were degassed for 4 min with a filament current setting of 5 and briefly fired before sample fracture. Replicas were picked up as described in¹⁸. Micrographs were taken at 10⁵X with a JEM 100 CM TEM equipped with EM-BSR a side entry goniometer and a 40 µm objective and a 200 µm condenser aperture, and an objective

focal length of 5mm.

Torus measurements were obtained from tracings of each object made with a Wild microscope fitted with a drawing tube. Circumferences were determined with a map contour measurer. Using a mirror-stereoscope with a light-dot-parallax device and the parallax equation of Nankivell,¹⁹ we measured the elevations of torus metal replica features relative to a fixed point on the ice surface in stereomicrographs (10° tilt) that had first been photographically contrast-reversed and printed for a stereoscopic final magnification of 10⁶X.

The maximum errors in the height measurements in Figure 6 were estimated using maximum error estimates in the measurements. The height uncertainty of the torus DNA strand points is between 0.03 Å and 24 Å and averages 13.6 Å ± 7.9 Å. These uncertainty values do not alter the relationship between the two DNA strands in Figure 6 and in future work these uncertainty values can be reduced substantially.

RESULTS

Frozen Hydrated Toruses in Spermidine-Condensed Calf Thymus DNA Preparations.

The formation of spermidine-condensed calf thymus DNA structures was detected by a simple sedimentation assay. Under the buffer conditions used in this freeze-etch EM study, the formation of spermidine-condensed calf thymus DNA is about half complete¹⁷. The spermidine-condensed DNA preparations contained other condensed structures in addition to toruses. However, toruses were the only regular geometric structures observed and, as such, proved easy to identify unambiguously by their shadow characteristics. Moreover, since these toruses represent an in vitro model system for bacteriophage or viral DNA head packaging²⁰ we have concentrated entirely in this study on the elucidation of torus substructure.

A group of representative hydrated spermidine-condensed calf-thymus DNA toruses is shown in Figure 1. In all cases, identification of the torus shape can be clearly made by the characteristic dark shadow region behind the front and rear torus annulus areas facing the Pt/C replication source. The unidirectional Pt/C source makes approximately a 45° angle to the overall specimen surface and is directed from the top of Figure 1 to the bottom in all its panels. The toruses in Figure 1 vary somewhat in size but all of them appear to be continuous around their entire

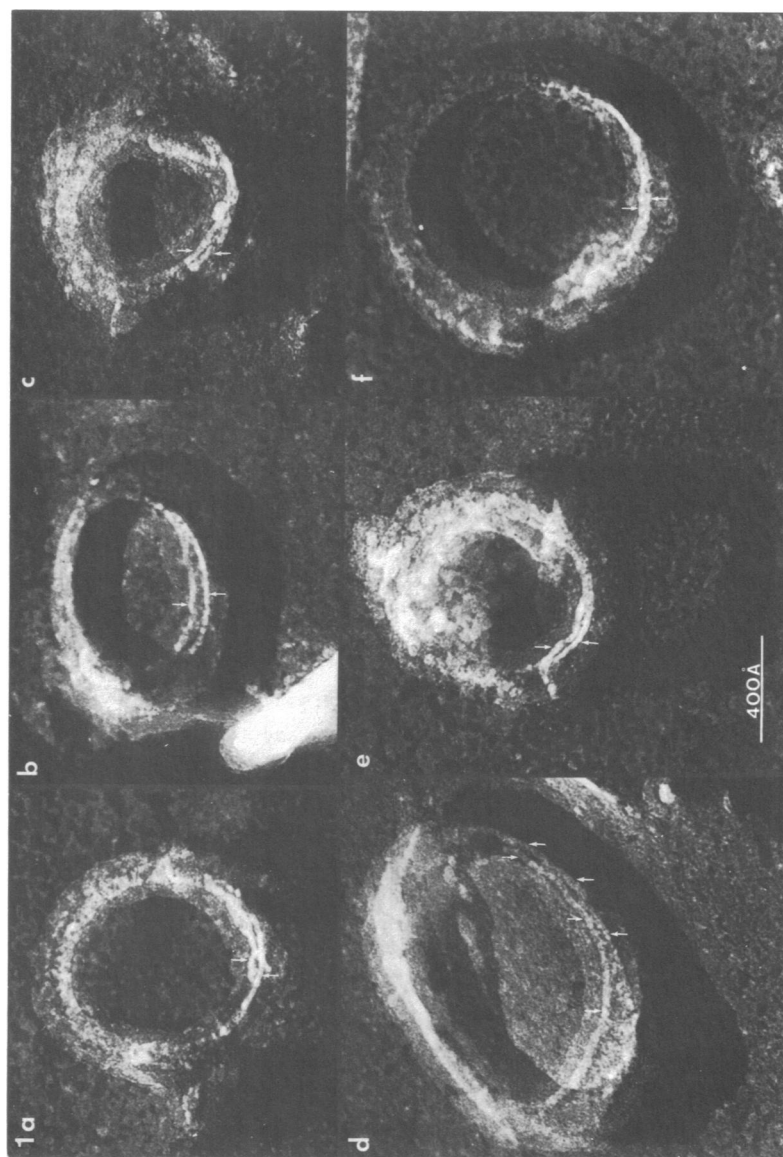


Figure 1. Spermidine-condensed calf thymus DNA toruses (a-f) visualized by freeze-etch electron microscopy. Single direction shadowing (from top to bottom) at a 45° angle with Pt/C (9 Å thick) has produced high contrast replicas highlighting the circumferential wrapping of surface DNA double helix fibres indicated by the white arrows. (bar=400 Å).

circumference. To date, we have found no evidence of torus-like DNA condensates or intermediates which have been formed by blunt-end-rod-fusion--a mechanism proposed in the literature⁷.

The other notable substructural feature of the Figure 1 objects is that Pt/C metal decoration has highlighted those torus surface features we believe to be double helical DNA strands wrapping circumferentially to form the torus (small arrows). We will return to this feature of torus organization later in the study.

Torus Dimensions

To gain some insight into the distribution of torus dimensions present in our preparation, we made the measurements presented in the following three figures on those toruses unambiguously defined by their shadow characteristics. Inner and outer circumference histograms are presented in Figure 2 where the measured values in Angstrom units have been converted into base pairs (bp) of circumferentially-wrapped B geometry DNA. Spermidine-condensed DNAs under these conditions have been shown by CD spectroscopy to have the B conformation²¹. Both distributions' average inner and outer circumference values with the 95 percent confidence intervals are shown in the histograms. The distributions themselves are rather broad, undoubtedly reflecting: 1) the heterogeneous calf thymus DNA fragment distribution and 2) some intermolecular aggregation of DNA double helices during collapse at the 5 $\mu\text{g}/\text{ml}$ condensing DNA concentration^{2, 11}. This latter factor would best explain why a few inner circumference values are found above 680 bp and why outer circumference values are larger than 900 bp. Finally, a contribution to each distribution spread may also be made by the lack of, or the kinetic inaccessibility of, a single thermodynamically-preferred torus dimension.

The inner and outer circumference values of a torus are linked parameters, as the data in Figure 3 show. A reasonable correlation (0.868) exists between the inner and outer circumference values although there is considerable scatter in the data. The best fit linear slope through the data is 0.935. A slope of less than one is expected for the relationship between these parameters assuming a simple, geometric model of a constant volume torus (with no intermolecular DNA aggregation). For this situation it can easily be shown that the outer circumference grows at a slower absolute rate than the inner circumference as the inner circumference is increased.

Measurements of horizontal torus ring thickness were performed. Only

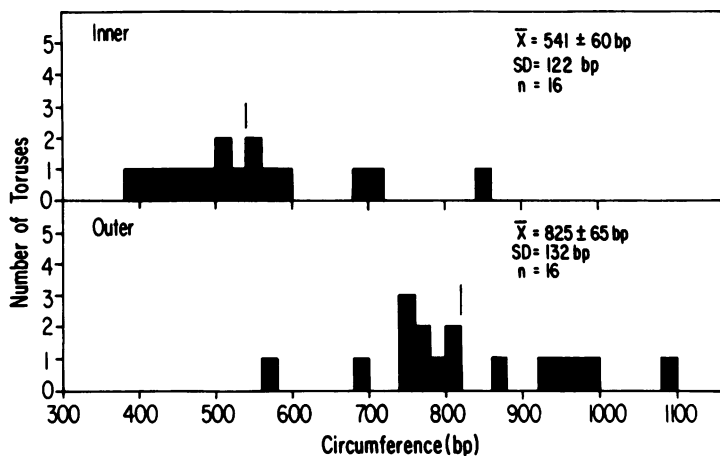


Figure 2. Histogram of inner and outer circumference values for a population ($n=16$) of spermidine-calf thymus DNA toruses. The values are given in base pairs (bp) of circumferentially wrapped B geometry DNA (3.4 Å/bp) for convenience in later discussion. The mean values (\bar{X}) with 95% confidence value are stated. Standard deviations (SD) are given for each circumference population. Since the correction for Pt/C increase in outer circumference and decrease in the inner circumference are within the error of making these measurements, these corrections have been ignored.

sections of toruses whose ring annuli axes ran parallel with the shadow direction were measured. The distribution yielded a shadowed mean value of 143 ± 18 Å. We estimate that the Pt/C metal increases the average thickness by 5-10 Å, which would result in a thickness of 133-138 Å. The

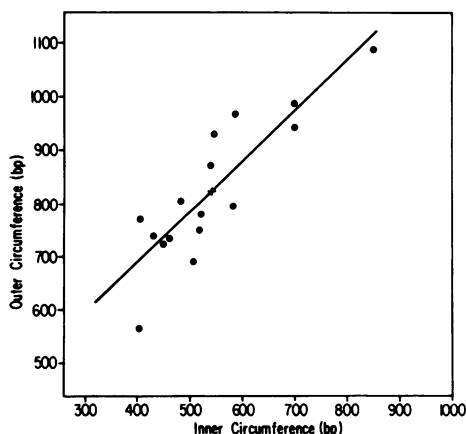


Figure 3. Correlation between inner and outer circumference values of the spermidine-calf thymus DNA torus population. A linear regression analysis of the data has the best fit line shown with slope = 0.935, intercept = 319 bp and correlation coefficient = 0.868. The symbol (+) marks the point defined by the Figure 2 mean inner and outer circumference.

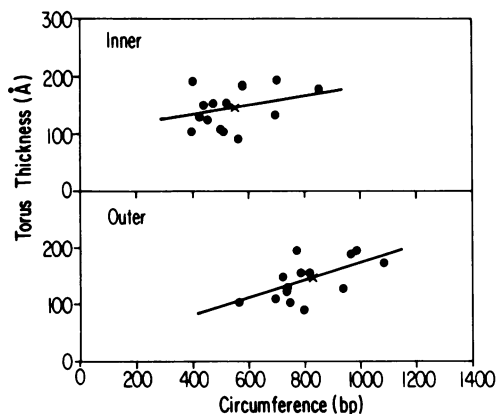


Figure 4. Torus thickness is plotted against the measured inner and outer torus circumference value. The thickness of each torus ring was measured exclusively in sections of torus oriented parallel to the shadow direction. This was done to ensure measurement of the entire evenly shadowed torus ring. Best fit linear regression lines are drawn. The fit data are as follows: Inner, slope = 0.081 Å/bp and correlation coefficient = 0.305; Outer, slope = 0.156 Å/bp and correlation coefficient = 0.610. The (X) markers indicate the points defined by the population mean parameters.

uncorrected and/or corrected thicknesses are in excellent agreement with the two-dimensional circumference measurements of Figure 3. When the inner and outer circumference data represented by the best fit line in Figure 3 are treated as circumferences of circles then an average torus thickness value of 143 Å can be calculated.

In Figure 4 the torus ring thickness values are plotted against the corresponding inner and outer torus circumference values. The scatter in these data is substantial and the best linear fit correlations are poor (0.305 and 0.610). However, the best linear fit slope for the outer circumference data is 0.156 Å/bp--twice that for the inner circumference data (0.081 Å/bp).

Stereoscopic Analysis of Toruses Reveals Circumferential DNA Wrapping

Valuable information has been obtained from stereomicrographs of spermidine-calf thymus DNA toruses concerning DNA double strand organization in both horizontal and vertical directions in these objects. Stereomicrograph pairs of two torus-shaped complexes with a tilt angle separation of 10° are shown in Figure 5. Using a stereoviewer it is quite

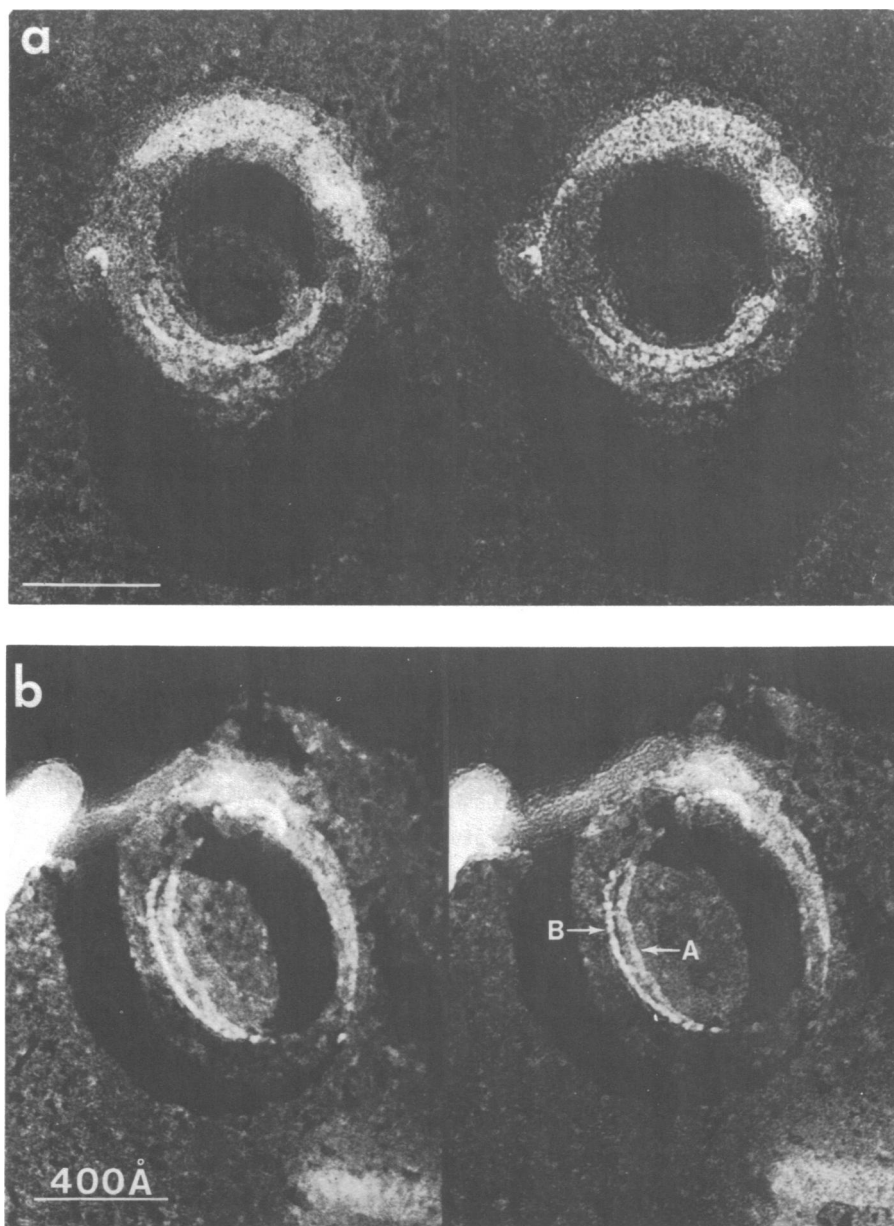


Figure 5. Stereomicrograph pairs of two spermidine-calf thymus DNA toruses (a, b). In panel (b) the higher lying DNA double helix fibre has been labelled A; the lower lying fibre is labelled B. Both panels (a) and (b) have a 10° tilt angle separation between the torus views shown. (Bar= 400 Å).

evident that both toruses possess a vertical dimension such that their upper surfaces lie well above the ice surface.

Substructural surface detail is evident in both objects. Metal decoration of continuous fibres running circumferentially along the torus ring axis is obvious at the inside rear surface. Similar DNA-strand decoration is evident in Figure 1. The toruses in both Figures 1 and 5 have surface decorated continuous fibres with widths in the 20-30 Å range. Considering that only 9 Å of Pt/C has been deposited onto these structures, the measured fibre widths are consistent with their being DNA double helices. Furthermore, in the Figure 5B torus, viewing with a stereoviewer confirms that the fibre labelled A lies suspended above the torus upper surface above fiber B. This argues rather strongly that these surface decorated features are continuous fibres arranged circumferentially about the torus. Specifically, this excludes the possibility that the metal-decorated features are aligned surface manifestations of periodic torus structure arranged at right angles to the torus ring.

The regular geometric appearance of the Figure 5 toruses and their surface fibre metal decoration detail suggests that torus organization consists of circumferentially-wound, well-ordered DNA helices. This appearance is somewhat deceptive since measurements reveal irregularity in the packing of these surface fibres. We performed height measurements on the Figure 5A torus stereomicrographs. Summarized in Figure 6 are the measured elevations in Angstrom units indicated relative to a fixed arbitrary zero point on the torus' lower fibre. The upper torus fibre elevations are marked with large asterisks; the lower torus fibre elevations are marked with small asterisks. First, it will be noted that the ice surface slopes downward to the right and the torus appears to be contacting the ice only at its left side close to the 136 Å ice measurement area. The torus is suspended well above the ice surface over most of its circumference. Measurements marked with large asterisks (198 Å, 37 Å, 113 Å, 152 Å, 128 Å) indicate the path of the upper DNA fibre from left to right about the torus ring. These data suggest that the torus surface, far from being flat, is likely to be puckered in the vertical direction. The lower-lying fibre, described by the small asterisk sequence (134 Å, 37 Å, 0 Å, 67 Å, 147 Å, 187 Å) from left to right, shows a topology in which the circumferentially-wrapped DNA double helix is initially on the bottom of the torus (134 Å, 37 Å, 0 Å). Within

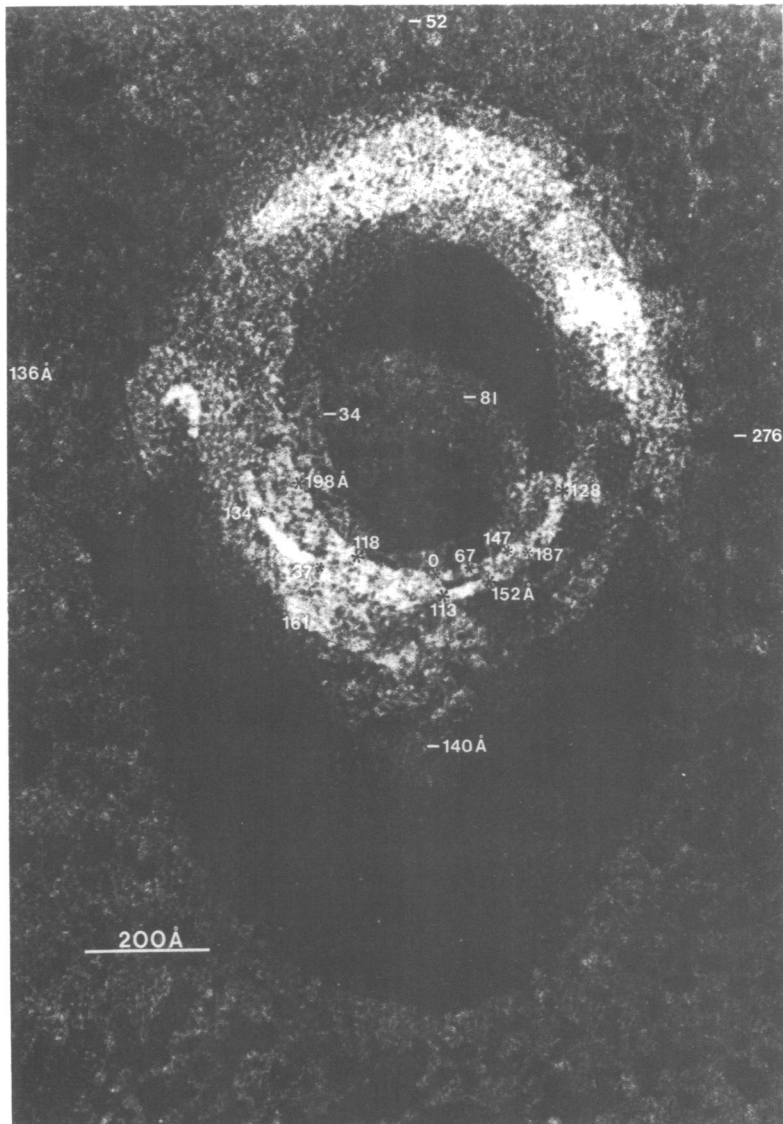


Figure 6. Summary of mirror stereoscope measurements on DNA topology in a spermidine-calf thymus DNA torus. A mirror stereoscope with a light-dot parallax device was used to measure the elevation of the decorated fibre positions shown (small * lower strand, large * upper strand) relative to a fixed arbitrary position 0A. All measurements are given in Å units. There was a 10° tilt angle between torus views (Figure 5a torus) and measurements were made on prints of the object at a final magnification 1,000,000. The error in these measurements is discussed in the materials and methods. (Bar = 200 Å).

the next 100 Å of apparent horizontal circumferential path, the DNA has risen close to 150 Å (0 Å, 67 Å, 147 Å). It then rises an additional 40 Å to 187 Å and crosses over the upper DNA strand.

DISCUSSION

All previous electron microscopic studies of condensed toruses discussed above have utilized preparation techniques that dehydrated the specimens. The present study was prompted by concern that surface tension forces during dehydration and exposure to solvents may have disrupted or rearranged specimen structure, and concern that torus substructure even if it could be seen in these studies, would not be meaningful. We have utilized freeze-etch electron microscopy to visualize frozen hydrated specimens decorated with very thin Pt/C replicas so that meaningful torus surface substructure could be visualized. From our studies we draw the following conclusions:

- 1) Toruses are not dehydration artifacts, since they exist under the solution-like conditions of the freeze-etch experiment.
- 2) Spermidine-calf thymus DNA toruses in our study have the following average dimensions expressed in Å units or bp of circumferentially wrapped B geometry DNA: inner circumference (1840 ± 204 Å or 541 ± 60 bp), outer circumference (2800 ± 222 Å or 825 ± 65 bp), torus ring thickness (143 ± 18 Å).
- 3) No constant length rod-like structures or toruses formed from bending rod-like structures were visualized in our hydrated spermidine-condensed DNA preparations.
- 4) In nearly every torus we visualized there were circumferentially-wrapping surface fibres having diameters in the 20-30 Å range, which suggests that they are actually double helical DNA strands and that the prevalent mode of torus organization is circumferential DNA wrapping.
- 5) The power to reveal macromolecular substructure by stereoscopic measurements on high magnification stereo-pairs of any biological structure has been demonstrated. A stereo-pair (tilt angle 10°) of one torus revealed the topological paths of two surface DNA double helices. The circumferential path of DNA seen in individual micrographs (Fig. 1) is apparently a general phenomenon, although minor exceptions may exist for surface DNA strands.

The above conclusions are embodied in the Figure 7 Torus Model. We propose a torus organized by continuous circumferential DNA wrapping. The electron microscopic evidence in this study and in biochemical studies on spermidine-condensed calf thymus toruses¹⁷ and the topologically-constrained spermidine-condensed ϕ x-174 RFII DNA torus system¹ argues for a continuous circumferential DNA-winding model. Our model incorporates a semi-crystalline hexagonal packing of DNA nearest neighbor helices. While this is obviously an idealized situation, there is reasonable evidence for hexagonal packing of DNA in bacteriophage heads, fibres, and crystals²⁰.

The torus dimensions in the Figure 7 model are those taken from the population statistical means. Values found in the literature for torus outer circumference range from 700 bp to 1700 bp^{4,6,8}. Differences in DNA size or spermidine-condensing concentration cannot account for this range of observed sizes. While torus preparation differences may be responsible for the large values of Allison et al.⁸ (equilibrium dialysis) compared to the other studies in which direct mixing was used, electron microscopy preparation technique differences must also be considered important. All reported techniques contained a sample dehydration step.

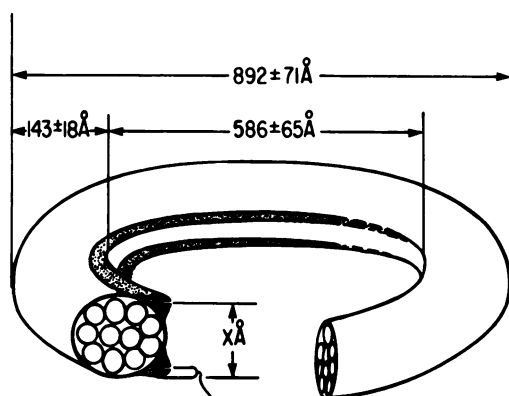


Figure 7. Model of DNA Torus organization by Continuous Circumferential wrapping of DNA. A largely hexagonally close-packed DNA torus ring is shown in cross-section where each DNA double helix is represented by one small circle and continuous circumferential wrapping of one long DNA double helix is sufficient to form the structure. The shaded areas represent an idealized description of the topological path of two surface DNA double helix fibres of the type measured in Figures 1 and 5a,b. Torus parameters indicated are those mean population values given in Figures 2-4. The torus ring thicknesses have not been measured so this dimension is indicated by the unknown X A.

DNA-spermidine complexes have been shown to undergo a reversible transition to the A geometry under low water activity conditions ²². This may help explain the smaller torus sizes. The low values of the Chatteraj et. al. ⁴ involved binding the toruses to cytochrome c or polylysine covered grids. Polylysine is known to interact strongly with DNA, producing condensed structures by its own action.¹² The visualization of torus structures has been shown by Chatteraj et. al. ⁴ to be very sensitive to the types of negative stain used and to the portion of grid surface area to which objects were attached.

The preparation uncertainties caused by dehydration, the application of solvents, and substrate surface are circumvented with the freeze-etch technique. Rapid freezing produces a situation in which objects are considered to be under solution-like conditions. The low temperature reached in the freeze-etch experiment should not significantly distort DNA in the complexes. Drew et. al. ²³ have shown no significant change in the 10.1 base pair/turn value of B geometry DNA on x-ray structure determination of a dodecamer crystal down to 16°K. Our samples probably remained hydrated even during the etching and replication steps because the vapor pressure of bulk ice should be greater than that of tightly-bound DNA water of hydration ^{18, 24}. The low Pt/C metal level used in our replicas is sufficient to provide high image contrast without burying or distorting major substructural features. Therefore, we feel that the torus dimensions and circumferential winding of surface DNA double helix fibres reported here more accurately reflects the solution DNA organization in these structures than other EM techniques.

Interestingly enough, Manning ²⁵ has developed a thermodynamic stability theory that predicts a critical minimum radius of curvature for DNA toruses. This value, $r = 170 \text{ \AA}$, represents an effective lower limit to the curvature of DNA due to the steeply rising repulsive potential energy of atomic packing. The corresponding lower limit to torus inner circumference is 315 bp. In this study 398 bp is our lowest measured value. Moreover, in another, more extensive freeze fracture study ($n = 72$ toruses), we have measured torus inner circumferences down to an abrupt 310 bp lower limit in a spermidine-condensed ϕ X-174 RF II DNA population. This is in excellent agreement with the theory and constitutes additional evidence supporting our contention that the freeze fracture technique yields information most relevant to the solution conformations of these objects.

In this study we have purposefully limited our scope to an examination of condensed DNA torus structure. The torus geometry, a predominant particle shape visualized in many electron microscopic studies of polycation-condensed DNA^{2-4, 6-9, 11,12}, is from a biological standpoint, the most important structure to study in these freeze-etch preparations. Although no simple packing model accounts entirely for DNA organization in bacteriophage or viral capsids²⁰ the double stranded DNA genomes of bacteriophage λ ⁴ and T4^{14,15} and of herpes simplex virus¹⁶ are thought to exist, condensed, in torus-like structures. The importance of the *in vitro* condensed DNA toruses lies in their function as model systems revealing principles of DNA organization that may operate in the biological pathogens. That polycation assisted condensation of pathogen DNA into torus-like structures may function in nature in systems like those mentioned above is suggested by the following observations. A modified base, α -putrescinylothymidine, replaces one-half of the thymine residues in the bacteriophage ϕ W-14 DNA^{26,27}. The α -putresciny group is a covalent polyamine dication modification of the thymine residue. It is thought that this covalent dication modification promotes DNA condensation into the virion head.

Spheroidal structures have also been seen in a number of the studies discussed^{4, 7} and there may be an equilibrium between these structures and toruses. Another structure reported in dehydrated spermidinecondensed DNA preparations is the constant length rod (about 2000 Å). This object has been proposed by Eickbush and Moudrianakis⁷ as a folding intermediate in the mechanism of torus formation by blunt-end-rod-fusion. We have noted a total absence of rod-like or constant length rod structures in our hydrated preparations. The electron microscopy of these investigators indicates the possibility that under totally dehydrating conditions toruses certainly may form by a blunt-end-rod-fusion mechanism. However, we see no evidence in our torus structures for such a mechanism and conclude that it does not represent a significant kinetic pathway for collapse in our preparations. We hope to extend our studies to freeze dried preparations where a complete and statistical examination of all aspects of the system becomes feasible.

The evidence against blunt-end-rod-fusion as a solution torus-formation mechanism is further strengthened by the micrococcal nuclease digestion study of Marx and Reynolds¹ on spermidine-condensed ϕ X-174 RF II DNA, the nicked, circular form. In this study, an arithmetic DNA band

series can be rationalized on topological grounds only in terms of a model torus organized by continuous, circumferential winding of DNA. A similar arithmetic series of broad DNA bands has been noted in gels when spermidine-condensed calf thymus DNA was digested with micrococcal nuclease ¹⁷. The monomer band in this study (760 ± 87 bp) is proposed to be the average length of DNA wound around one complete circumferential turn of the torus. Therefore, the average torus, comprised of a collapsed monomer DNA molecule (13×10^6 d) would be organized by about 25 circumferential DNA wraps of 760 ± 87 bp. This circumferential wrap value is intermediate in magnitude between the mean torus inner circumference (541 ± 60 bp) and mean torus outer circumference (825 ± 65 bp) measured in this study. Thus, these freeze-etch electron microscopic data agree well with independent biochemical results in support of a model for torus organization in which DNA is circumferentially wound in a single direction and most likely is hexagonally-closepacked in a semi-crystalline array to comprise the torus interior.

ACKNOWLEDGEMENTS

K.A.M. acknowledges support from: Grant Number CA23108, National Cancer Institute, DHEW; Grant Numbers, GM25886 and AI17586, National Institute of Health, DHEW; Research Corporation Grant 8859 and Biomedical Research Support Grant RR-05392. G.C.R. acknowledges support from CA23108, National Cancer Institute, DHEW.

*To whom reprint requests should be addressed.

REFERENCES

1. Marx, K.A. and Reynolds, T.C. (1982) Proc. Nat'l. Acad. Sci. USA, 79, 6484-6488.
2. Widom, J. and Baldwin, R.L. (1980) J. Mol. Biol. 144, 431-453.
3. Gosule, L.C. and Schellman, J.A. (1976) Nature 259, 333-335.
4. Chatteraj, O.K., Gosule, L.C. and Schellman, J.A. (1978) J. Mol. Biol. 121, 327-337.
5. Campbell, R.A. et al., eds. (1979) "Advances in Polyamine Research", Vol. 1, Raven Press, New York.
6. Skuridin, S.G., Kadykov, V.A., Shashkov, V.S., Evdokimov, Yu. M. and Varshavski, Ya. M. (1978) Mol. Biol. (Moscow) 12, 413-420.
7. Eickbush, T.H. and Moudrianakis, E.N. (1976) Cell 13, 295-306.
8. Allison, S.A., Herr, J.C. and Schurr, J.M. (1981) Biopolymers 20, 469-488.
9. Ruben, G.C., Marx, K.A. and Reynolds, T.C. (1981) Proceedings of the 39th Annual Meeting Electron Microscope Society of America--Atlanta, GA, G.W. Bailey, Ed. Claitor's Publishing Division, Baton Rouge, LA, p.438-439.

10. Ruben, G.C., Marx, K.A. and Reynolds T.C. (1981) Proceedings of the 39th Annual Meeting Electron Microscope Society of America--Atlanta, GA, G.W. Bailey, ed. Claitor's Publishing Division, Baton Rouge, LA, p 440-441.
11. Wilson, R.W. and Bloomfield, V.A. (1979) *Biochemistry* 18, 2192-2196.
12. Hsiang, M.W. and Cole, R.D. (1977) *Proc. Nat'l. Acad. Sci. USA*, 74, 4852-4856.
13. Manning, G.S. (1978) *Quart. Rev. Biophys.* 11, 179-246.
14. Klimenko, S.M., Tikhonenko, T.I. and Andreev, V.M. (1967) *J. Mol. Biol.* 23, 523-533.
15. Richards, K.E., Williams, P.C. and Calendar, R. (1973) *J. Mol. Biol.* 78, 255-259.
16. Furlong, D., Swift, H. and Roizman, B. (1972) *J. Virol.* 10, 1071-1074.
17. Marx, K.A. and Reynolds, T.C., submitted for publication.
18. Ruben, G.C. and Telford, J.N. (1980) *J. Microscopy*, 118, 191.
19. Nankivell, J.F. (1963) *Optik*, 20, 172.
20. Earnshaw, W.C. and Casjens, S.R. (1980) *Cell* 21, 319-331.
21. Gosule, L.C. and Schellman, J.A. (1978) *J. Mol. Biol.* 121, 311-326.
22. Huse, Y.H., Mitsui, Y., Iitaka, Y., Miyaki, K. (1978) *J. Mol. Biol.* 122, 43-53.
23. Drew, H.R., Samson, S. and Dickerson, R.E. (1982) *Proc. Nat'l. Acad. Sci. USA*, 79, 4040-4044.
24. Kellenberger, E. and Kistler, J. (1979) In: *Advances in Structural Research by Diffraction Methods*, 7, pg. 73 (W. Hoppe and R. Mason, eds) Friedr. Vieweg & Sohn Braunschweig/Wiesbaden.
25. Manning, G.S. (1980) *Biopolymers*, 19, 37-59.
26. Kropinski, A.M.B., Bose, R.J. and Warren, R.A.J. (1973) *Biochemistry* 12, 151.
27. Gerhard, B. and Warren, R.A.J. (1982) *Biochemistry* 21, 5458-5462.